Adaptive Whole-Arm Grasping Approach of Tumbling Space Debris by Two Coordinated Hyper-redundant Manipulators

Wenya Wan[1], Chong Sun[1(✉)], Jianping Yuan[1], Xianghao Hou[1], Yufei Guo[1], Yinong Ou-yang[1], Qixin Li[1], Liran Zhao[1], Hao Shi[2], and Dawei Han[3]

[1] National Key Laboratory of Aerospace Flight Dynamics, Northwestern Polytechnical University, 127 West Youyi Road, Beilin District, Xi'an, Shaanxi, China
sunchong@nwpu.edu.cn
[2] North Automatic Control Technology Institute, Sports Road No. 351, Xiaodian District, Tai Yuan, Shanxi, China
[3] Aerospace System Engineering Shanghai, Shanghai, China

Abstract. Space debris generally has unknown motion information, which brings great challenge for space debris capture and removal. In this paper, we propose an adaptive whole-arm grasping approach of tumbling space debris by two coordinated hyper-redundant manipulators. Firstly, the dynamic model of the tumbling target is derived and its motion characteristics are analyzed. Secondly, a complementary grasping strategy is proposed for tumbling space debris capture, in which two coordinated hyper-redundant manipulators are utilized to wrap around the space debris together. The grasping strategy includes two steps (1) determining the twining curve for each hyper-redundant manipulator and (2) searching algorithm for feasible grasping configuration that could match with the twining curve. Specifically, the second step involves the capture occasion determination and the pre-planning technique. The main advantages of the proposed method lie in its grasping efficiency and adaptivity to grasped objects. Finally, two examples to verify the effectiveness of the proposed method are presented.

Keywords: Space debris capture · Coordinated hyper-redundant manipulators · Complementary grasping strategy · Twining curve

1 Introduction

The Earth orbit is in a serious predicament caused by millions of space debris. Operational satellite vital for mankind infrastructure are threatened to be destroyed by space debris. Thus, active debris removal is of great relevance [1]. However, most space debris are in the tumbling state and there are not any handles to be grasped on these un-controlled objects, which makes the capture and removal of space tumbling targets more challenging.

H. Yu et al. (Eds.): ICIRA 2019, LNAI 11740, pp. 450–461, 2019.
https://doi.org/10.1007/978-3-030-27526-6_39

Space robotics is considered as one of the most promising approaches for on-orbit servicing missions such as docking, repairing and orbital debris removal [2]. Robotic arm technology has been applied in many on-orbit servicing missions [3–7]. According to the number of arms, it can be divided into single-arm capture [3, 4] and multi-arm capture [6, 7]. Compared with a single-arm space robot, a dual-arm or multi-arm system has much more dexterity and flexibility, and can complete more complex tasks [6]. However, the existing researches mainly focus on utilizing the end-effector located at the tip of arms to grasp the target where grappling points are required. As a result, the variety of grasped objects is limited.

Unlike the capture using fingertips, whole-arm capture can be more adaptive and can provide better grasping efficiency. Vividly, the whole-arm capture is carried out by wrapping the arms and torso around an object, which is in the same manner as an octopus [8]. Early work on robotic whole-arm capture started in 1988 [9], but has not received much interest until recently [10–13]. In terms of the whole-arm capture, the ratio of object size to robot size is larger which is useful in many applications especially those involving hazardous environments such as search and rescue, underwater and space exploration [10, 11]. Devereux's work developed methods that allowed serial chained manipulators to explore, analyze and plan whole arm grasps for a wide variety of objects [12]. Anders used methods from continuous-state reinforcement-learning to solve for whole-arm grasping policies [13].

Borrowing experiences from whole-arm capture, an adaptive whole-arm grasping approach of space tumbling targets by two coordinated hyper-redundant manipulators is presented in this paper, in which the grasping handles are not required and the variety of grasped objects is allowed. We first analyze the motion characteristics of the tumbling space debris. Then, a complementary grasping strategy is proposed mainly including the determination of the twining curve, the optimal capture occasion determination and grasping configuration design based on rapidly-exploring random tree (RRT) algorithm [14]. The main advantages of the proposed method lie in its grasping efficiency and adaptivity to grasped targets.

The remainder of this paper is organized as follows. Section 2 establishes the attitude motion model of the tumbling target, and analyzes its motion characteristics. In Sect. 3, the grasping strategy and grasping configuration design algorithm are presented. An example to verify the effectiveness of the proposed method is shown in Sect. 4. Finally, the conclusive remarks are given in Sect. 5.

2 Analysis of an Un-controlled Spacecraft

There are no requirements for the geometry of grasped objects as our proposed approach encircles around the object's surface to grasp it. Besides, the size of the grasped object is determined by the given specific manipulators' length. Further, the orbital motion between the grasped object and the servicing satellite system usually is synchronous, and the relative distance between the grasped object and the hyper-redundant manipulator is very small, which means that we could only focus on the caging motion of the hyper-redundant manipulator. Therefore, the analysis of an un-controlled spacecraft can focus on its attitude motion.

2.1 Dynamic Modeling of an Un-controlled Spacecraft

Under the action of space perturbation moments, most space debris often exhibit complex tumbling motion, which brings difficulties to the implementation of active debris removal mission. The possible rotation patterns of space debris can be divided into three groups: spin motion around the minimum axis of inertia I_z, spin motion around the maximum axis of inertia I_x, and the tumbling motion with nutation angle. Assume the external toque acted on the target is $\boldsymbol{\tau} = [\tau_x, \tau_y, \tau_z]^{\mathrm{T}}$, its equation of motion satisfies Eq. (1).

$$\begin{cases} I_x\dot{\omega}_x - I_{xy}\dot{\omega}_y - I_{xz}\dot{\omega}_z + (I_z - I_y)\omega_y\omega_z - I_{yz}(\omega_y^2 - \omega_z^2) - I_{xz}\omega_x\omega_y + I_{xy}\omega_x\omega_z = \tau_x \\ I_y\dot{\omega}_y - I_{xy}\dot{\omega}_x - I_{yz}\dot{\omega}_z + (I_x - I_z)\omega_x\omega_z - I_{xz}(\omega_z^2 - \omega_x^2) - I_{xy}\omega_y\omega_z + I_{yz}\omega_x\omega_y = \tau_y \\ I_z\dot{\omega}_z - I_{xz}\dot{\omega}_x - I_{yz}\dot{\omega}_y + (I_y - I_x)\omega_x\omega_y - I_{xy}(\omega_x^2 - \omega_y^2) - I_{yz}\omega_x\omega_z + I_{xz}\omega_y\omega_z = \tau_z \end{cases} \tag{1}$$

here, $\boldsymbol{I} = [I_x, I_{xy}, I_{xz}; I_{xy}, I_y, I_{yz}; I_{xz}, I_{yz}, I_z]$ and $\boldsymbol{\omega} = [\omega_x, \omega_y, \omega_z]^{\mathrm{T}}$ are the inertia and angular velocity of the target in the frame *oxyz*, respectively. The attitude transformation matrix $\boldsymbol{A}(\boldsymbol{q})$ from the target's fixed frame *oxyz* to the inertial frame is as follows:

$$\boldsymbol{A}(\boldsymbol{q}) = \begin{bmatrix} q_0^2 + q_1^2 - q_2^2 - q_3^2 & 2q_1q_2 - 2q_0q_3 & 2q_1q_3 + 2q_0q_2 \\ 2q_1q_2 + 2q_0q_3 & q_0^2 - q_1^2 + q_2^2 - q_3^2 & 2q_2q_3 - 2q_0q_1 \\ 2q_1q_3 - 2q_0q_2 & 2q_2q_3 + 2q_0q_1 & q_0^2 - q_1^2 - q_2^2 + q_3^2 \end{bmatrix} \tag{2}$$

where, $\boldsymbol{q} = [q_0, \hat{\boldsymbol{q}}]^T = [q_0, q_1, q_2, q_3]^T$ is the unit quaternion representing the target's attitude, whose derivative are the functions of $\boldsymbol{q}$ and $\boldsymbol{\omega}$:

$$\begin{bmatrix} \dot{q}_0 \\ \dot{q}_1 \\ \dot{q}_2 \\ \dot{q}_3 \end{bmatrix} = \frac{1}{2}\begin{bmatrix} -q_1 & -q_2 & -q_3 \\ q_0 & -q_3 & q_2 \\ q_3 & q_0 & -q_1 \\ -q_2 & q_1 & q_0 \end{bmatrix}\begin{bmatrix} \omega_x \\ \omega_y \\ \omega_z \end{bmatrix} = \frac{1}{2}\mathbf{S}(\boldsymbol{q})\boldsymbol{\omega} \tag{3}$$

For an arbitrary point on the target, its position vector in body-fixed frame and inertial frame are respectively denoted by $\boldsymbol{r}_a^t$ and $\boldsymbol{r}_a^I$ satisfying following relationship:

$$\boldsymbol{r}_a^I = \boldsymbol{A}(\boldsymbol{q})\boldsymbol{r}_a^t \tag{4}$$

2.2 Analysis of an Un-controlled Spacecraft

In real cases, the space target could be affected by external perturbations. However, since external forces/torques acting upon a free-floating object in space are usually small, it is reasonable here to assume that the target in space is free from any external forces and torques. Assume the grasped target is a cube with side length 0.7 m and it rotates along the principal axes of inertia, the initial attitude quaternion is $\boldsymbol{q}_0 = [1, 0, 0, 0]^{\mathrm{T}}$, the mass of the target is $m_t = 929.53$ kg, the inertia matrix is $\boldsymbol{I} = diag(75.912,$

75.912, 75.912) (kg m^2), and the initial angular velocity of the tumbling target is $\omega_0 = [2, 1, 1]^T$ (°/s). According to the theoretical calculation, the 3D trajectory of an arbitrary point or close curve of the grasped target during 500 s is shown in Fig. 1.

According to the results, the trajectory of an arbitrary point on the surface of space debris targets is a circle, but the trajectory of a closed curve is more complex. Therefore, the tumbling space targets capture by traditional point capture is difficult.

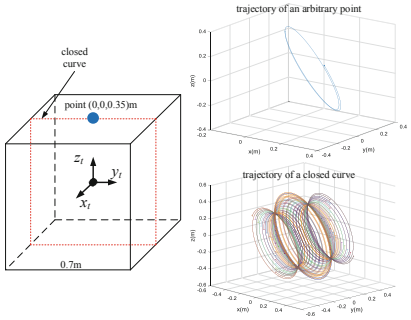

Fig. 1. The 3D trajectory of an arbitrary point and close curve of the grasped target.

3 Grasping Approach by Two Coordinated Hyper-redundant Manipulators

3.1 Grasping Strategy

In this paper, a complementary grasping strategy is proposed for the capture of space tumbling targets, in which the two coordinated hyper-redundant manipulators use their own whole arm to wrap around the grasped target together. The flow chart of the whole-arm grasping strategy is shown in Fig. 2.

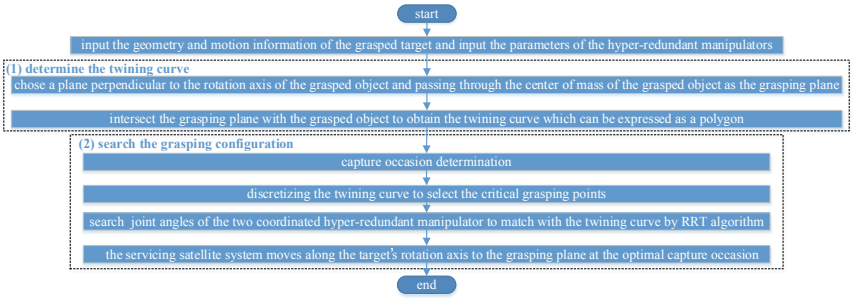

Fig. 2. The flow chart of the whole-arm grasping strategy.

The grasping strategy includes two main steps: the first step is to determine the twining curve, and the second is to search a feasible grasping configuration that could match with the twining curve by two coordinated hyper-redundant manipulators. In terms of the first step, there are two concrete sub-steps: (1) randomly chose a plane perpendicular to the rotation axis of the grasped object and passing through the center of mass of the grasped object as the grasping plane; (2) intersect the grasping plane with the grasped object to obtain the twining curve which can be expressed as a polygon. The black and red dotted lines in Fig. 3 represent the grasping plane and twining curve, respectively. In practice, the grasping plane usually is chosen as the plane determined by the two hyper-redundant manipulator to reduce the maneuver of the servicing satellite. As for the second step, RRT algorithm is adopted too search joint angles of the two coordinated hyper-redundant manipulator that can match with the twining curve. We will discuss how to plan a path for the two coordinated hyper-redundant manipulators that can realize the grasping configuration in detail in the following sections.

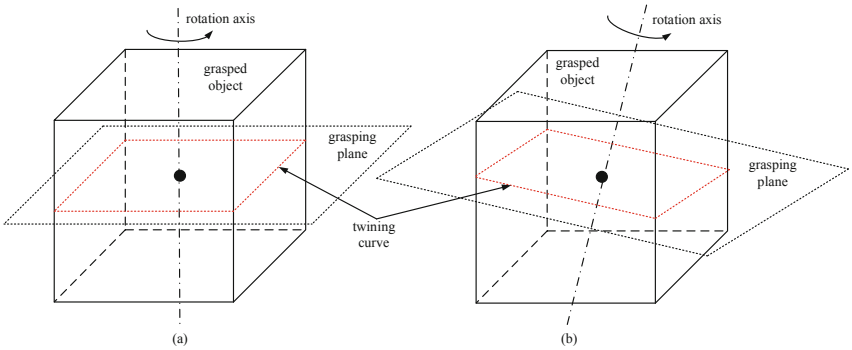

Fig. 3. Illustration of the determination of the twining curve where (a) and (b) are the cases where the grasped object rotates around the principal inertia axis and an arbitrary axis, respectively. (Color figure online)

3.2 Grasping Configuration Design

In this subsection, the kinematic motion equations of a dual-arm space robot is derived first; then the grasping configuration searching algorithm is designed.

The Kinematic Motion Equations of a Dual-Arm Space Robot

A two coordinated hyper-redundant manipulators is used to capture a tumbling target. The space robotic system is composed of a robot base, a n_1-link serial manipulator (called arm-1) and a n_2-link serial manipulator (called arm-2). Further, the universal joint structure with two orthogonal degree of freedoms (DOFs) is adopted in this paper. The model is shown in Fig. 4.

For convenience of discussion, some symbols are defined in Table 1. The coordinate transformation matrix between two adjacent coordinate frame $O_j\ x_j\ y_j\ z_j$ and $O_{j-1}\ x_{j-1}\ y_{j-1}\ z_{j-1}$ of arm-i (i = 1, 2) can be expressed in Eq. (5). Here, Trans(x, y, z)

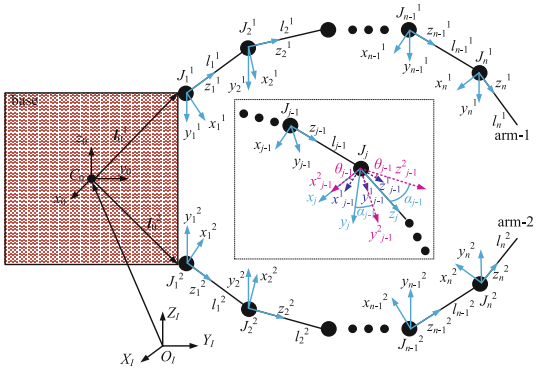

Fig. 4. A general model of the two coordinated hyper-redundant space robot system.

Table 1. Some important symbols used in this paper.

Symbol	Representation
C_0	The mass center of the base
l_0^i	The vector from C_0 to the first joint J_1 of arm-i, i = 1, 2
J_j^i	The jth joint of arm-i, i = 1, 2, j = 1, 2, … , n_i
l_j^i	The length of the jth link of arm-i, i = 1, 2, j = 1, 2, … , n_i
θ_j^i	The rotation angle about y_j axis of the jth joint of arm-i, i = 1, 2, j = 1, 2, … , n_i
α_j^i	The rotation angle about x_j axis of the jth joint of arm-i, i = 1, 2, j = 1, 2, … , n_i
$O_I\ X_I\ Y_I\ Z_I$	The inertial coordinate system
$C_0\ x_0\ y_0\ z_0$	The fixed coordinate system of the base
$O_j^i\ x_j^i\ y_j^i\ z_j^i$	The fixed coordinate system of the jth joint and link of arm-i, i = 1, 2, j = 1, 2, … ,n_i
${}^i\boldsymbol{T}_j$	The coordinate transformation matrix from $O_j\ x_j\ y_j\ z_j$ to $O_i\ x_i\ y_i\ z_i$

is the translational transfer matrix; Rot(y, θ) is the rotational transfer matrix around the y axis; and Rot(x, α) is the rotational transfer matrix around the x axis. Further, the pose (position and attitude) of the jth link arm-i ${}^1T_j^i$ can be obtained according to Eq. (6).

$$
\begin{aligned}
{}^{j-1}\boldsymbol{T}_j &= \mathrm{Trans}(0,0,l_{j-1}) \cdot \mathrm{Rot}(y_{j-1}^1, \theta_{j-1}) \cdot \mathrm{Rot}(x_{j-1}^2, \alpha_{j-1}) \\
&= \begin{bmatrix}
\cos\theta_{j-1} & \sin\theta_{j-1}\sin\alpha_{j-1} & \sin\theta_{j-1}\cos\alpha_{j-1} & 0 \\
0 & \cos\alpha_{j-1} & -\sin\alpha_{j-1} & 0 \\
-\sin\theta_{j-1} & \cos\theta_{j-1}\sin\alpha_{j-1} & \cos\theta_{j-1}\cos\alpha_{j-1} & l_{j-1} \\
0 & 0 & 0 & 1
\end{bmatrix}
\end{aligned} \tag{5}
$$

$$ {}^{I}\boldsymbol{T}_{j} = {}^{I}\boldsymbol{T}_{0}{}^{0}\boldsymbol{T}_{1}{}^{1}\boldsymbol{T}_{2}\cdots{}^{j-1}\boldsymbol{T}_{j-2}{}^{j-1}\boldsymbol{T}_{j} \tag{6} $$

Grasping Configuration Searching Algorithm Based on RRT Algorithm

The two coordinated hyper-redundant manipulators work together to realize the match of the twining curve as shown in Fig. 5. In the beginning, the links are straightened out ready to be twining around the target. Then, the manipulators sweep around the entire target by adjusting the joint orderly from the most proximal joint to the most distal joint.

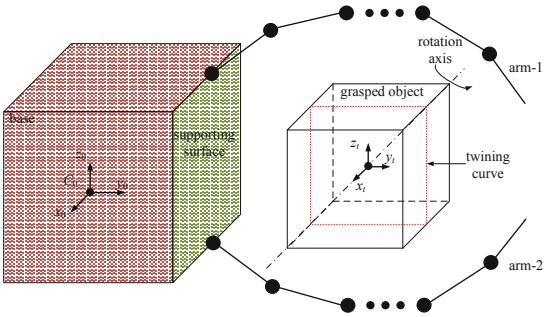

Fig. 5. Task description of grasping a tumbling space target by the two coordinated hyper-redundant manipulators.

Assume the hyper-redundant manipulators have been located in a plane parallel to the grasping plane before starting the grasping operation which can be obtained easily by adjusting the torsion angle of the first universal joint. Besides, the hyper-redundant manipulators could arrive at the grasping plane rapidly when the optimal capture occasion occurs. Then, the problem can be simplified to the planar grasping problem. Given that the twining curve is movable along with the grasped target, to grasp the target firmly, the capture occasion determination and the pre-planning technique are included in our proposed grasping configuration searching algorithm.

Capture Occasion Determination

Considering the capture of a tumbling target should be safe and reliable, the occasion where the attitude synchronization of the serving satellite and the grasped target is achieved, is chosen as the alternative occasion. In other words, the relative attitude of the twining curve to the servicing satellite is **0** when the capture is implemented, just as the configuration shown in Fig. 5. Further, taking account of the rapidity of the capture, the first or the second synchronous occasion is usually chosen as the optimal capture occasion according to the initial relative attitude as shown in Fig. 6. Therefore, we can plan the joint angles according to the state of the twining curve at the optimal capture occasion in advance.

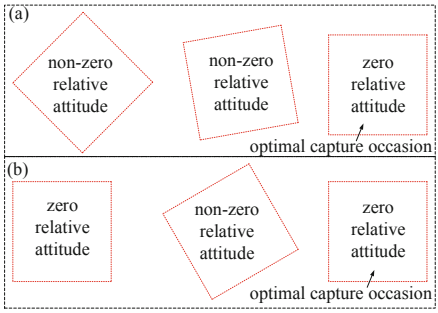

Fig. 6. Illustration of the capture occasion determination: (a) and (b) are cases where the first and the second synchronous occasion are selected as the optimal capture occasion, respectively.

Pre-planning Technique Based on RRT Algorithm

In the beginning, the critical grasping points are selected by discretizing the twining curve. As shown in Fig. 7, the critical grasping points are usually chosen as the vertexes of the twining curve to guarantee a firm capture; besides, an additional critical grasping point is selected on the wrapping demarcation edge of the twinning curve as the wrapping demarcation point of two hyper-redundant manipulators. It must be pointed out the whole-arm capture will take advantage of the surface of the base of the satellite system that is directly facing the grasped target (for example, the surface marked reseda in Fig. 5), and this surface works as a supporting surface during the grasping process. Then, the critical grasping points are divided into two groups for the two hyper-redundant manipulators bounded by the wrapping demarcation point. Now, the problem is how to realize the match of the corresponding critical grasping points for the two hyper-redundant manipulators independently while simultaneously.

Specifically, the proposed method attempts to find valid connections between two adjacent critical grasping points by RRT algorithm as shown in Table 2. The inputs of the algorithm are the joint number that coincides with the first critical grasping point j_s^i, the total number of critical grasping points for arm-i k^i, the link number of arm-i n^i, the initial configuration of arm-i $\boldsymbol{q}_{\text{ini}}^i$, the link length l_j^i, the joint angle range $\theta_j^i \in \left[\theta_{jl}^i, \theta_{ju}^i\right]$ and $\alpha_j^i \in \left[\alpha_{jl}^i, \alpha_{ju}^i\right]$. The output of the algorithm is the joint angles $\boldsymbol{q}$ of the valid grasping configuration. A connection is valid if the manipulator can move between the two adjacent critical grasping points with a positive integral number of links and without breaking the joint angle limitation. A connection between two adjacent critical grasping points attempts to increase the number of links until the number is greater than a user specified maximum or a connection is successful. This process continues until either the algorithm has planned a path around the entire circumference of the twining curve.

The grasping configuration is calculated in advance, and the hyper-redundant manipulator has adjusted its configuration from the initial configuration to the grasping configuration before the optimal capture configuration occurs. Then, the hyper-redundant manipulators move along the target's rotation axis to the grasping plane when the optimal capture configuration occurs. Finally, the tumbling space target can be grasped firmly.

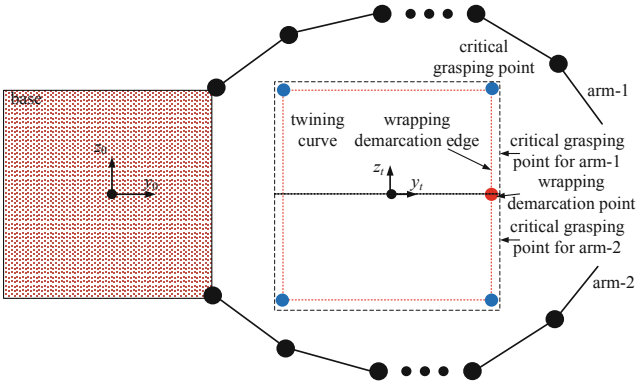

Fig. 7. Illustration of the pre-planning technique.

Table 2. Procure of grasping configuration searching algorithm based on RRT algorithm.

Step	Content
1	Input j_s^i, k^i, n^i, $\boldsymbol{q}_{\text{ini}}{}^i$, $l_j{}^i$, $\theta_j{}^i \in [\theta_{jl}{}^i, \theta_{ju}{}^i]$, $\alpha_j{}^i \in [\alpha_{jl}{}^i, \alpha_{ju}{}^i]$ where i=1,2, set the rand seeds number N
2	For i^i=1:k^i-1
3	j=j_s^i
4	While j<=n^i
5	For N^i<=N
6	Set an initial value of the j_s^i th~jth joints←$\boldsymbol{q}_{\text{ini}}$
7	Generate a random configuration $\boldsymbol{q}_{\text{rand}}$
8	Find the nearest configuration $\boldsymbol{q}_{\text{near}}$ in the current configuration path branches
9	Generate a candidate of new configuration $\boldsymbol{q}_{\text{cand}}$ located between $\boldsymbol{q}_{\text{rand}}$ and $\boldsymbol{q}_{\text{near}}$
10	Examine whether the hyper-redundant manipulators collide with the object; when no collision is detected, $\boldsymbol{q}_{\text{cand}}$ becomes a new configuration $\boldsymbol{q}_{\text{new}}$ and be added to the configuration path branches
11	Check if the jth joint with joint values $\boldsymbol{q}_{\text{new}}$ could match with the i^i th critical grasping points; if a valid match is found: $\boldsymbol{q}(j_s^i{:}j)$= $\boldsymbol{q}_{\text{new}}$, j_s^i=j, go to line 2
12	End
13	If a valid match is found: $\boldsymbol{q}(j_s^i{:}j)$= $\boldsymbol{q}_{\text{new}}$, j_s^i=j, go to line 2
14	End
15	End
16	Output the joint angles $\boldsymbol{q}$ of the valid grasping configuration

4 Simulations

The structure configuration of the simulation example is shown in Fig. 5, which consists of two 11-universal-joint manipulators mounted on a free-floating servicing satellite and a tumbling space target. Further, assume the base of the servicing satellite system is a cube with side length 1 m, each link of the hyper-redundant manipulator is same with length $l = 0.2$ m, and the joint angles range is also same satisfying $\theta \in [-180°, 180°]$ and $\alpha \in [-180°, 180°]$. The grasped targets are two cubes with angular velocity is $\boldsymbol{\omega} = [2°, 0°, 0°]$. Then, the simplified model is shown in Fig. 7. Further, assume the initial time $t_0 = 0$ s. In addition, all the initial joints angles of the two hyper-redundant manipulator are $\alpha_{j0}^{i} = 0°$ and $\theta_{j0}^{i} = 0°$ ($j = 1, 2, \ldots, 11$ and $i = 1, 2$).

Case 1: the cube with side length $a = 0.7$ m
In this case, the size of the grasped target is smaller than the base of the servicing satellite system. Assume the initial relative attitude between the grasped target and the servicing satellite is $\boldsymbol{A} = \mathrm{Rot}(x, -30°)$. Thus, the first synchronous occasion is chosen as the optimal capture occasion just as the case shown in Fig. 6(a). The capture time $t_f = 165$ s, which means that there are 165 s for the servicing satellite system to calculate the grasping configuration. The process of one possible grasping configuration design is shown in Fig. 8. The joint angles $\alpha_{j0}^{i} = 0°$ ($j = 1, 2, \ldots, 11$ and $i = 1, 2$) which coincides with the planar grasping case. As for the joint angles rotating around the y axis are shown in Table 3. Then, the servicing satellite system moves along the target's rotation axis to the grasping plane at the optimal capture occasion as shown in Fig. 9.

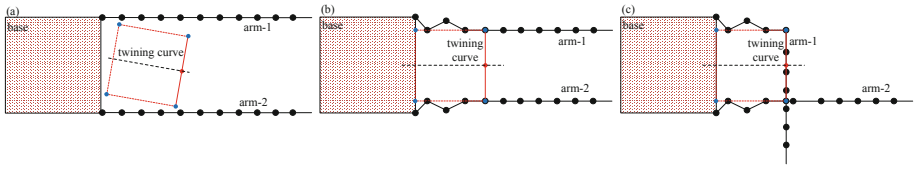

Fig. 8. The process of one possible grasping configuration design for Case 1where (a), (b) and (c) are the initial configuration, the middle configuration and final grasping configuration, respectively.

Case 2: the cube with side length $a = 1.2$ m
In this case, the size of the grasped target is larger than the base of the servicing satellite system. Assume the initial relative attitude between the grasped target and the servicing satellite is $\mathbf{0}$. Thus, the second synchronous occasion is chosen as the optimal capture occasion just as the case shown in Fig. 6(b). The capture time $t_f = 180$ s. The process of one possible grasping configuration design is shown in Fig. 10. The joint angles $\alpha_j^i = 0°$ ($j = 1, 2, \ldots, 11$ and $i = 1, 2$) and the joint angles rotating around the y axis are shown in Table 4. Then, the servicing satellite system also moves along the target's rotation axis to the grasping plane, which is similar to the process shown in Fig. 9.

Table 3. Joint angles rotating around the y axis for Case 1.

Arm	$\theta_1(°)$	$\theta_2(°)$	$\theta_3(°)$	$\theta_4(°)$	$\theta_5(°)$	$\theta_6(°)$	$\theta_7(°)$	$\theta_8(°)$	$\theta_9(°)$	$\theta_{10}(°)$	$\theta_{11}(°)$
1	48.59	−71.77	46.36	−23.18	90	0	0	0	0	0	0
2	48.59	−71.77	46.36	−23.18	0	0	0	0	0	0	0

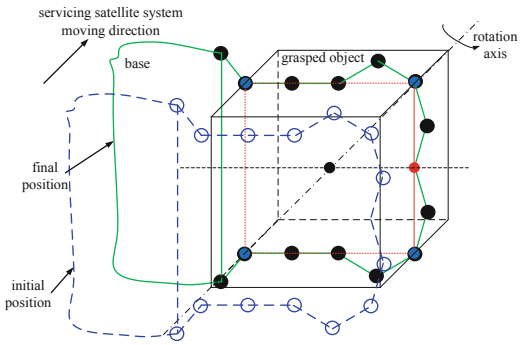

Fig. 9. Illustration of the achievement of the final grasping configuration.

In addition, It must be pointed out that our proposed method is also applicable for 3-dimensional capture because the universal joint has two orthogonal DOFs.

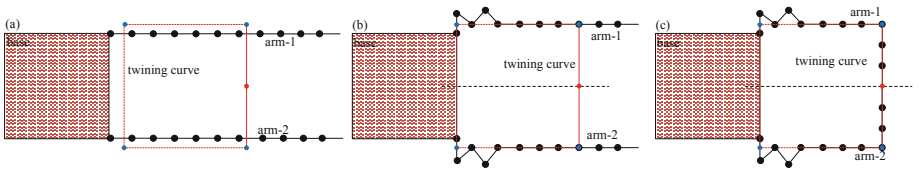

Fig. 10. The process of one possible grasping configuration design for Case 2 where (a), (b) and (c) are the initial configuration, the middle configuration and final grasping configuration, respectively.

Table 4. Joint angles rotating around the y axis for Case 2.

Arm	$\theta_1(°)$	$\theta_2(°)$	$\theta_3(°)$	$\theta_4(°)$	$\theta_5(°)$	$\theta_6(°)$	$\theta_7(°)$	$\theta_8(°)$	$\theta_9(°)$	$\theta_{10}(°)$	$\theta_{11}(°)$
1	−90	120	−85.46	110.92	−55.46	0	0	0	90	0	0
2	−90	120	−85.46	110.92	−55.46	0	0	0	90	0	0

5 Conclusions

In this paper, an adaptive whole-arm grasping approach of tumbling space debris by two coordinated hyper-redundant manipulators is proposed. Firstly, we has analyzed a space un-controlled target' motion characteristics based on its dynamic modeling.

Then, a complementary grasping strategy is proposed for the capture of space tumbling targets. Using proposed approach, it can determine the twining curve and search a feasible grasping configuration that could match with the twining curve using rapidly-exploring random tree. To verify the effectiveness of the proposed method, examples of failed Cube-Sat capture are presented to verify the proposed method, and the simulation results have shown that the grasped targets can be grasped firmly. In future, the grasping path planning and control will be studied.

Acknowledgment. This Research was supported by National Natural Science Foundation of China (No. 11802238).

References

1. Shan, M., Guo, J., Gill, E.: Review and comparison of active space debris capturing and removal methods. Prog. Aerosp. Sci. **80**, 18–32 (2016)
2. Flores-Abad, A., Ma, O., Pham, K., et al.: A review of space robotics technologies for on-orbit servicing. Prog. Aerosp. Sci. **68**, 1–26 (2014)
3. Reintsema, D., Thaeter, J., Rathke, A., et al.: DEOS—the German robotics approach to secure and de-orbit malfunctioned satellites from low earth orbits. In: Proceedings of the i-SAIRAS, Sapporo, Japan (2010)
4. Debus, T.J., Dougherty, S.P.: Overview and performance of the front-end robotics enabling near-term demonstration (FREND) robotic arm. In: AIAA Aerospace Conference, Reston, VA, USA (2009)
5. Chong, S., Jianping, Y., Wenya, W., Yao, C.: Outside envelop grasping method and approaching trajectory optimization for tumbling malfunctional satellite capture. Acta Aeronauticaet Astronautica Sinica **39**(11), 322192–322203 (2018)
6. Peng, J., Xu, W.W., Pan, E.Z., et al.: Dual-arm coordinated capturing of an unknown tumbling target based on efficient parameters estimation. Acta Astronautica (2019)
7. Ellery, A.: A robotics perspective on human space flight. Earth Moon Planets **87**(3), 173–190 (1999)
8. Walker, I.D., Dawson, D.M., Flash, T., et al.: Continuum robot arms inspired by cephalopods. In: Proceedings of SPIE-The International Society for Optical Engineering, vol. 5804, pp. 303–314 (2005)
9. Salisbury, K.: Whole arm manipulation. In: International Symposium on Robotics Research. MIT Press (1988)
10. Braganza, D., Mcintyre, M.L., Dawson, D.M., et al.: Whole arm grasping control for redundant robot manipulators. In: American Control Conference. IEEE (2006)
11. Oki, T., Nakanishi, H., Yoshida, K.: Whole-body motion control for capturing a tumbling target by a free-floating space robot. In: Proceedings of the 2007 IEEE/RSJ International Conference on Intelligent Robots and Systems. IEEE, San Diego (2007)
12. Devereux, D.: Control strategies for whole arm grasping. The University of Manchester (2010)
13. Anders, A.: Learning a strategy for whole-arm grasping. Massachusetts Institution of Technology (2014)
14. LaValle, S.M.: Rapidly-exploring random trees: a new tool for path planning. TR98–11, Department of Computer Science, Iowa State University (1998)